

MODELING OF THE SURFACE MICROCRACKING IN POLYETHYLENE DUE TO UV-DEGRADATION

Ihor Skrypnyk^{1,2)}, Jan Spoormaker²⁾, Natalia Bilyk¹⁾

¹⁾Karpenko Physico-Mechanical Institute, National Academy of Sciences of Ukraine, Lviv, Ukraine

²⁾Delft University of Technology, Delft, the Netherlands

ABSTRACT

The long outdoor service of polymeric materials is limited by their degradation. The oxidation processes, which occur there, induce significant changes in the polymers' structure: chain' scission, cross-linking, additional crystallization of amorphous regions, etc. These phenomena severely impact the strength of the amorphous zones in polymers at surface, thus making material brittle.

Although the chemical and morphological aspects of these processes as well as their impact on mechanical properties are thoroughly studied, the problem of prediction of mechanical behavior of degraded material is far from its solution. A net of microcracks nucleate along the amorphous zones, which (in fact) are main objects for environmental degradation of polymers. These microcracks covers the surface of the strongly degraded polymer, providing stress concentrators and channels for oxygen transport into bulk material. The manifold of microcracks, the diversity of their location and shapes, make the consideration of this problem within the frameworks of fracture mechanics practically impossible.

In this paper, a simplified approach for modeling of the surface microcracking due to ultra-violet degradation (UV-degradation), based on the percolation theory, is proposed. The main elements of the methodology of computer simulation on the Voronoi tessellation are presented.

The methodology is applied to study the surface cracks evolution in high-density polyethylene assisted by UV-degradation. The scale effect of surface microcracking is studied. Two possible reasons for scale effect are discussed: the ration of crystallite size to the scale of a whole solid and the characteristic size of internal stresses within the polymer, induced by additional crystallization in process of environmental degradation. It is shown, that scale effect does not influence the shape factor of microcrack clusters, but does influence the microcrack rate development.

INTRODUCTION

Photo-oxidation (otherwise called "ultraviolet-degradation") is one of the main mechanisms of environmental degradation of polymers [1, 2]. It is commonly accepted that the scheme of chain auto-oxidation of free radicals plays here the main role. It results in polymeric chains' scission [2, 3], as well as their cross-linking [2, 4, 5]. Both processes reduce the mechanical strength of the amorphous zone between the crystalline lamellae in a polymer. As a result, the strain at failure of a polymer decreases significantly (fig. 1a), i.e. material becomes brittle.

The mechanical behavior of ultraviolet-degraded (UV-degraded) polymeric specimens and structural elements is also studied in details [6-9]. Since the auto-oxidation requires constant replenishment of oxygen in material from surface, the spatial distributions of solved oxygen (as well as of the products of oxidation

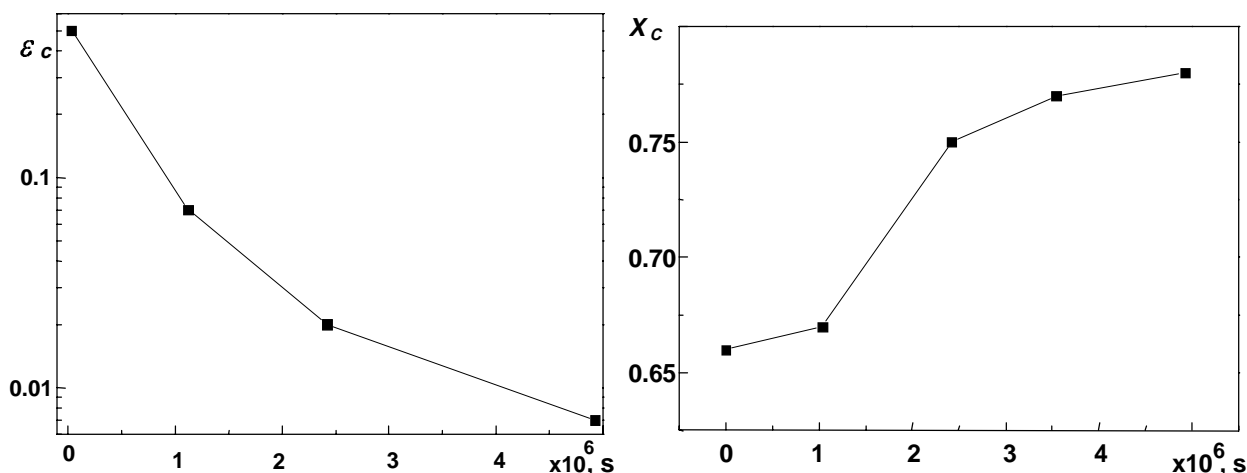


Figure 1: Strain failure, (a) and crystallinity X_c (weight fraction), (b) versus time of exposure to UV-radiation for 0.2mm HDPE film. Strain at failure registered for tension rate $3 \cdot 10^{-6} \text{ s}^{-1}$, [10].

reactions) are formed. Thus, the near-surface regions in polymers are most subjected to the UV-degradation. As a results, the tests, performed on the degraded polymeric parts, report the mechanical behavior of composite material, which is brittle near surface and ductile in the bulk.

Special experimental methodology [8-11], based on the testing of microfilms, cut out of degraded polymer, is used to study the performance of uniformly degraded polymers on the mesoscale. Still, these data relate to the performance of the entire microfilm sample. At the same time, visual observations show that mechanical behavior of polymer at the surface is non-homogeneous also on the smaller scale: for the strongly degraded material a net of microcracks covers the surface, providing stress concentrators and channels for easy oxygen transport into bulk material. These microcracks initiate along the amorphous zones, which (in fact) are main objects for environmental degradation of polymers. There are two reasons for such localization: first, the crystalline lamellae are impenetrable for oxygen [1]; secondly, the chromophores, which are able to absorb sunlight, are displaced from crystallites during the crystallization [12] into amorphous region.

The fracture mechanics approach is not effective for prediction the behavior of these microcracks. The microcrack' net covers the whole surface. The microcracks are very shallow (0.2 ... 0.4 mm). In addition, the layer, which is under the near-surface (cracked) region, is less degraded and, hence, much more ductile. Therefore, the propagation of microcracks into bulk material is restricted, until this layer will be adequately degraded, what is controlled by oxygen diffusion and kinetic constants of the chain auto-oxidation reaction.

In this paper, a simplified approach to modeling of the evolution of the surface microcracks' net, based on the percolation theory, is proposed.

SOME PHYSICO-CHEMICAL ASPECTS OF UV-ASSISTED CRACKING OF HDPE

As mentioned before, environmental degradation of semi-crystalline polymers leads to embrittlement [8, 9] and surface cracking. Latter can occur even for the polymeric parts that are not mechanically loaded. According to the concept of critical deformation $\varepsilon = \varepsilon_c$, there should be some internal stresses in the near-surface region, which would result in the deformation that overcome the critical level ε_c , in order for a microcrack to initiate.

There are two main reasons for internal stresses to appear: manufacturing process and weathering itself. Although the internal stresses, caused by manufacturing, create serious problem in everyday engineering practice, the problem can be solved, if the mould and cooling-down regime are designed properly. The environmentally induced internal stresses cannot be avoided, if the degradation process occurs. Therefore, here we consider the environmentally induced internal stresses as a driving force for surface cracking. The initiation of these internal stresses is due to change of polymer' crystallinity during the environmental degradation [9, 13]. The example of crystallinity' evolution in 0.2 mm HDPE film during UV-degradation test is presented in fig. 1b.

Since the density of HDPE crystalline phase ($\rho_c=1.001 \cdot 10^6 \text{ g/m}^3$) is higher, than that of amorphous phase ($\rho_a=0.856 \cdot 10^6 \text{ g/m}^3$) [14], the crystallinity growth leads to rise of total density of degraded material, which can be calculated as follows [9]:

$$\rho_{tot} = \frac{\rho_c \rho_a}{\rho_a X_c + \rho_c (1 - X_c)}. \quad (1)$$

Assuming that the mass growth of polymeric material due to oxidation is small, the increase in density should lead to drop in volume of degraded polymer. Because, degraded material near the surface is tied with material in the bulk, which is much less degraded, there will be a growing difference in the volume of near-surface regions and bulk material. This phenomenon is often called as "shrinkage due weathering". Then, change in time of the first strain invariant for the near-surface layer can be written:

$$\varepsilon_0(t) = [V_0 - V(t)]/V_0. \quad (2)$$

Here V_0 is the original volume (and the constant volume of bulk material, linked to considered part of surface); $V(t)$ denotes the variation of volume of degraded surface layer due to shrinkage. The decrease in volume of near-surface material leads, therefore, to rise of stresses. Taking into account the above assumption about the stability of polymer mass during weathering and, that the volume of a whole part consists of volume of amorphous and crystalline parts, the eqn. (2) can be rewritten as follows:

$$\varepsilon_0(t) = 1 - \frac{(1 - X_c(t)) \rho_c + X_c(t) \rho_a}{(1 - X_c(0)) \rho_c + X_c(0) \rho_a}. \quad (3)$$

Increasing of the material' straining near the surface (due to weathering) and drop of critical strain at failure leads to local failure (local microcracking along the intercrystalline region), when the deformation criterion holds: $\varepsilon_c(t_c) = \varepsilon_0(t_c)/3$. From this condition the critical time t_c , when the surface would be covered by the net of microcracks, can be estimated.

On the other hand, the surface cracking does not occur at one moment: spatial distribution of the crystallinity in polymer leads to variation of internal stresses. The material, which initially features higher crystallinity, does not have potential for large crystallinity growth (because crystallinity cannot be higher than 1). Thus, the gained internal stresses (strains) also would be lower. Assuming proportional change in crystallinity of different parts of material, the local crystallinity of arbitrary part of near-surface layer can be presented:

$$X_c(t) = X_c(0) + \frac{(1 - X_c(0))}{(1 - \bar{X}_c(0))} [\bar{X}_c(t) - \bar{X}_c(0)]. \quad (4)$$

These expressions create background for simulation of microcrack' net evolution.

ELEMENTS OF THE METHODOLOGY OF PERCOLATION SIMULATIONS

Percolation theory [15, 16] is an interdisciplinary field of research that constitutes mathematical apparatus for the theory of critical phenomena and phase transitions [17]. It studies the properties of spatial lattices, which rise as the collective properties of its elements.

For percolation simulations of damage evolution the “possibility to fail” is assumed and assigned to every element in considered lattice. This property can be related (through the probability distribution) to a certain parameter of microstructure, the field of local stresses, or linked with a micromechanism of fracture. Using random numbers seed this “possibility to fail” is drawn for every element. In other words, an "elementary failure act" is drawn based on some information about microstructure and using random numbers seed. Next, clusters (i.e. sets of connected “failed” elements), their properties and evolution are to be monitored. In this way the percolation approach enables to model the effect of microstructure and fracture' micromechanism on the behavior of the solid as a whole. Further, the lattice is scanned for a "percolation cluster", which connects two opposite sides of the studied lattice. If such cluster forms, it means that the lattice (i.e. "the solid") is split by that cluster into two parts. The probability of formation of percolation cluster (and corresponding "percolation thresholds" of microstructural parameters etc.) is to be monitored.

In order to simulate the surface cracking of semi-crystalline polymer, the Voronoi tessellation (fig. 3) was chosen as the geometrical representation of the material surface. The principle of formation of this geometrical object is accordant to the principles, which constitute the formation a of polycrystalline solid.

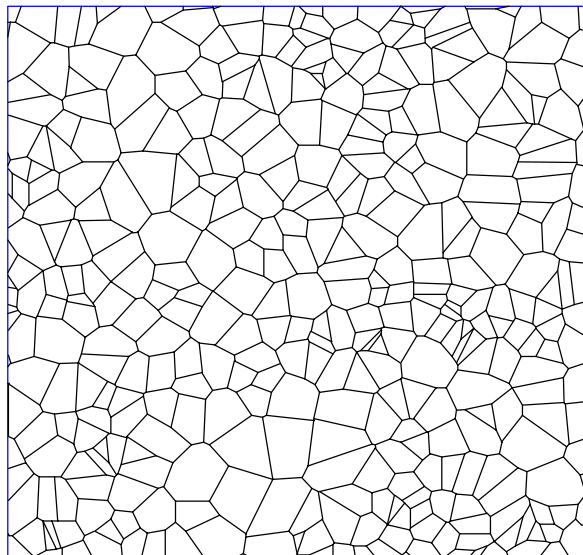


Figure 3: The Voronoi tessellation' scheme.

From the methodological point of view the use of stochastic lattices (like the Voronoi tessellation) required review of certain methodological aspects of computer percolation simulations as well as remake of program codes. The stochastic character of both – studied lattices and percolation modeling itself implies numerous computer simulation tests. Thus, the computation time for the single simulation test becomes important. In order to cut it down, the methodology of programming was based on the operations on lists of variables (data). From this point of view, the monitored clusters could be treated as the lists of their elements with varying (increasing) length. Merging two clusters would mean merging (adding) the lists of their elements into one new list.

For speeding up these operations, the lists of "neighbor elements" for every element were created. Since the "neighborhood"-relation involves two elements, this stage of modeling requires $\sim N^2$ operations for the stochastic lattice with the capacity of N elements. However, taking into account a simple fact, that the neighbor elements can't be located far away from each other (since they should have one common node), enable to decrease the amount of calculations considerably. Subdividing the studied Voronoi tessellation into

$m \times m$ squares and searching for the neighbor for arbitrary element only within the square where this element is located allows to create the "neighbor lists" after $\sim N + 0.5(N/m)^2$ operations (Table 1).

TABLE 1. COMPUTATION TIME FOR FORMATION OF "NEIGHBOR LISTS"

Number of elements in tessellation	Traditional approach	Subdividing of the Voronoi tessellation by			
		10x10	30x30	50x50	100x100
1050	170 ^{*)}	22 ^{*)}			
4300	1 550	130	87		
12800	12 700		390	369	
62700	272 000				5400

^{*)} Computation time for processor Pentium-II/233, given in seconds.

Further cut down of computation time can be reached if to account for the independence of "elementary failure acts". This allows to perform repeated computation tests for the same Voronoi tessellation by increasing gradually the probability of "possibility to fail" for arbitrary element. This enables to monitor clusters step-by-step, increasing their list of elements by those elements that fail during current simulation step. This approach is more efficient from the point of view of the time spent (Table 2) and it better reflects the process of damage evolution.

TABLE 2. COMPUTATION TIME FOR THE SERIES OF 20 TESTS, PERFORMED ON PENTIUM-II/233

Stage of simulation	Single test approach, s	Step-by-step modeling, s
Formation of the Voronoi tessellation (2000 elements)	90	90
First step of simulation	55	55
Subsequent steps	-	4
Computation time for the complete series of 20 tests	20 x (90+55) = 2900	90+55+19 x 4 = 221

Since the size of the Voronoi tessellation (or, more precisely, number of facets in the tessellation) influences the results of percolation simulation (scale effect), it is worth to perform the simulation for a set of meshes of different size. Next, using specific extrapolation technique [16], the conclusions concerning the behavior of infinitely large lattices can be derived. In the other words, the scale effect, related to the geometric peculiarities of the studied object, can be distinguished [17, 18].

The fluctuations due to misfit, created by shrinkage of a single crystallite, diminishes on a certain distance, which not necessary is of the order of magnitude of crystallite. This distance is related to another linear scale λ of the internal stress-strain field, which describes "waves", created by interactions of neighbor crystallites. To estimate the scale λ , following scheme can be considered. A spherical rigid insertion of radius r_0 is plugged into a void of spherical elastic solid of radius R , creating misfit δV . Then, the strains in radial direction are:

$$\varepsilon_{rr} = \frac{\delta V}{4\pi r^3} \left(C \left(\frac{r}{R} \right)^3 - 2 \right) / \left(C \left(\frac{r_0}{R} \right)^3 + 1 \right); \quad C = \frac{4G}{3K}. \quad (5)$$

Here G and K denote the shear and bulk moduli, correspondingly. The evaluation for the long-range characteristic scale λ can be obtained, while estimating the distance r , where the strains are decreased significantly (for instance, consist $\chi \varepsilon_{rr}(r_0)$ with $\chi = 0.01 \dots 0.05$). Simple transformations give:

$$r = \left[\chi \left(r_0^{-3} - 0.5CR^{-3} \right) + 0.5CR^{-3} \right]^{\frac{1}{3}}. \quad (6)$$

For typical values $R \sim 100 \dots 1000r_0$ (wall thickness of the plastic structural element) and $C \approx 0.3478$ the expression (6) gives: $\lambda \Big|_{\chi=0.01} \approx 4.6r_0$; $\lambda \Big|_{\chi=0.05} \approx 2.7r_0$.

The information on the long-range characteristic scale is useful for building simulation scheme. Crystallinity factor is the collective quality of the crystallites and can't be regarded to a single crystallite. On the other hand, regarding this factor to the whole solid would make no sense for percolation simulations. Therefore, the above estimated long-range scale λ serves as a characteristic range for calculation of the initial local crystallinity in material. Considering the region of $\lambda \times \lambda$ -size, the initial balance between amorphous and crystalline part can be written as follows:

$$(\delta l_i)/\lambda^2 + X_{ci}(0) = (\delta \bar{l})/\lambda^2 + \bar{X}_c(0) = 1, \quad (7)$$

where \bar{l} is the average length of amorphous zones over all $\lambda \times \lambda$ -regions; l_i is the length of amorphous zones for i region and $X_{ci}(0)$ denotes initial crystallinity for this region; δ is the width of amorphous zone. Expelling δ from the equations (7), one arrives:

$$X_{ci}(0) = 1 - (1 - \bar{X}_c(0))l_i/\bar{l}. \quad (8)$$

MODELING AND RESULTS

The following mesh' sizes were used for simulations in order to expel the influence of the tessellation size: 460; 1100; 4200; 12700 and 63000. Since the Voronoi tessellation contains certain probabilistic information, new Voronoi tessellation was generated for every computer simulation. All together 188 series of computer simulation were performed, each containing from 10 to 30 percolation tests (in this way 2590 records were accumulated for subsequent analysis).

Based on the data, accumulated, several parameters were monitored. Among others cluster capacity S_j (number of elements in an arbitrary j -cluster), j -cluster radius (also known as "radius of gyration" [16]):

$$\mathfrak{R}_j = \frac{1}{S_j} \sum_i \left[(Y_i - Y_0)^2 - (X_i - X_0)^2 \right]; \quad Y_0 = \frac{1}{S_j} \sum_i Y_i; \quad X_0 = \frac{1}{S_j} \sum_i X_i, \quad (9)$$

can be mentioned. Here X_i, Y_i are the coordinates of center of i -facet in cluster.

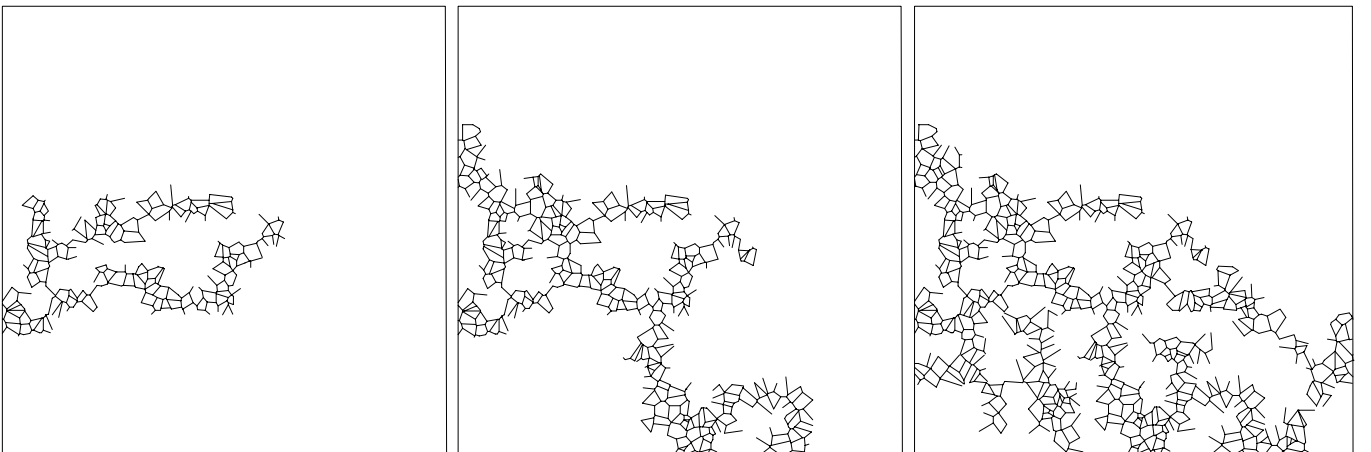


Fig. 4. Gradual formation of the percolation cluster in the Voronoi tessellation during the simulation of UV-degradation in HDPE.

Next, the distributions of number of clusters n_s (of capacity S) were calculated for every simulation step, when data were collected. In addition the average cluster radius \mathfrak{R}_{S_i} for the clusters of certain capacity S were calculated:

$$\mathfrak{R}_{S_i} = \frac{1}{n_{S_i}} \sum_j \mathfrak{R}_j . \quad (10)$$

The dependencies of the average cluster radius Eqn. (10) versus cluster capacity are plotted for several moments t_i of simulation and different mesh capacities L on fig. 5. They can be fairly fitted by straight parallel lines in log-log coordinates. Only for small clusters' these dependencies deviate from straight lines. However, the regular character of all deviations indicates, that these fluctuations are related to the long-scale effect of crystallinity. Thus, the diversity of generated cluster forms and Voronoi tessellations does not impact the $(\mathfrak{R}_S \sim S_i)$ dependency: while growing, the clusters “develop” according one tendency. The two sets of $(\mathfrak{R}_S \sim S_i)$ dependency for different time moments, but the same mesh capacity L , coincide. The $(\mathfrak{R}_S \sim S_i)$ dependencies for different L do not much, but for large S can be presented by single relation:

$$\mathfrak{R}_S (S, L) \approx F(L) S^\alpha ; \alpha \sim 1. \quad (11)$$

Unlike this, the evolution dependencies for cluster size in time (Fig. 6) for simulations with different mesh capacity L have even more sophisticated character. They look very much like the dependencies for percolation probabilities, presented in [18].

Therefore, it can be summarized, that growth rate $\dot{\mathfrak{R}}_S$ of the surface microcracking due to UV-degradation features strong scale effect. This conclusion is concordant with the well know fact, that the kinetic of small cracks cannot be described within the linear elastic fracture mechanics and depends on the scale of the solid, which contains small cracks.

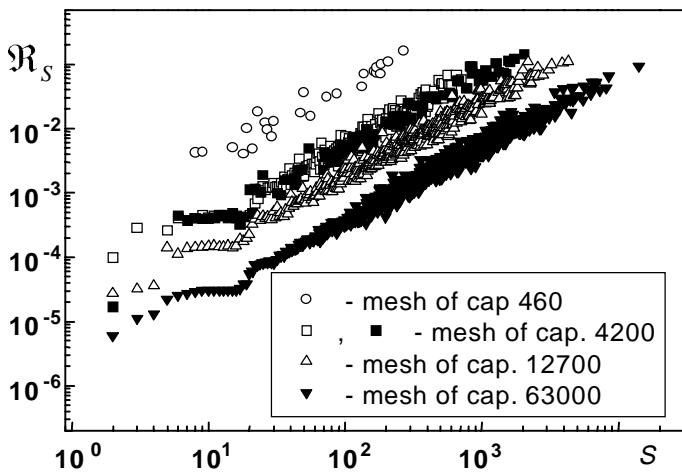


Fig. 5. Dependencies of averaged cluster radius \mathfrak{R}_S vs. cluster capacity S for different sizes of Voronoi tessellation, $\lambda = 3$.

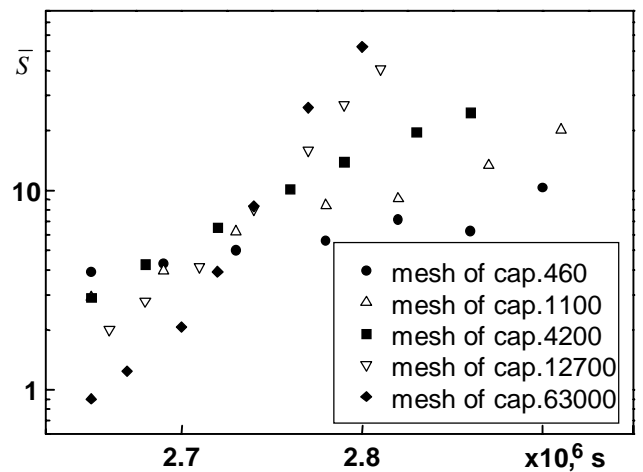


Fig. 6. Evolution of averaged cluster capacity \bar{S} in time for the simulations with meshes of different size.

REFERENCES

1. Garton A., Carlsson D.J., Wiles D.M. (1980) In: *Developments in polymer photochemistry*, Vol. 1, Chapter 4. – N.S. Allen (Ed.) – London: Appl. Sci. Publ.
2. Vink P. (1983) In: *Degradation and stabilization of polyolefins*, Chapter 5. – N.S. Allen (Ed.) – London: Appl. Sci. Publ.

3. Al-Malaika S., Scott G., (1983) In: *Degradation and stabilization of polyolefins*, Chapter 7 – N.S. Allen (Ed.) – London: Appl. Sci. Publ.
4. Langlois V., Meyer M., Audouin L., Verdu J. (1992) *Polym. Degr. Stab.* **36**, 207.
5. Henman T.J. (1983) In: *Degradation and stabilization of polyolefins*, Chapter 2 – N.S. Allen (Ed.) – London: Appl. Sci. Publ.
6. Banai E., Bezur L. (1974) *Int. Polym. Sci. Techn.* **1**, T/42.
7. Komitov P.G. (1989) *Polym. Degr. Stab.* **24**, 313.
8. Brujin J.C.M. de (1992) *The failure behaviour of high density polyethylene with an embrittled surface layer due to weathering*, Ph.D. Thesis, TU Delft, the Netherlands.
9. Hoekstra H.D. (1997) *The mechanical behavior of UV-degraded HDPE: Consequences for Designers*, Ph.D. Thesis, TU Delft, the Netherlands.
10. Brujin J.C.M. de, Meijer H.D.F. (1991) *Rev. Sci. Instrum.* **62**, 1620.
11. Suzuki S., Nishimura O., Kubota H. et al (1980) In: *23rd Japan congress on mechanical research – Non-metallic materials*.
12. Rabek J.F. (1987) *Mechanism of photophysical processes and photochemical reaction in polymers – Theory and applications* – Chichester: John Wiley & Sons.
13. Bhateja S.K. (1982) *Polym. Comm.* **23**, 654.
14. Moy F.H., Kamal M.P. (1980) *Polym. Eng. Sci.* **20**, 957.
15. *Percolation Structures and Processes* (1983) G. Deutscher, R. Zallen and J. Adler (Eds.), Annals of Israel Physical Society, **5**.
16. Stauffer D. (1985) *Introduction to percolation theory* – London: Taylor&Fransis.
17. Stanley H.E. (1971) *Introduction to phase transitions and critical phenomena* – Oxford University Press.
18. Skrypnyk I.D. (1997) *Exploration and exploitation of oil and gas wells*, **34**, 128 (In Ukrainian).